

# Ultrafast dynamical process of Ge irradiated by the femtosecond laser pulses

Fangjian Zhang<sup>1,2</sup>, Shuchang Li<sup>1,2</sup>, Anmin Chen<sup>1,2</sup>, Yuanfei Jiang<sup>1,2</sup>, Suyu Li<sup>1,2</sup>, and Mingxing Jin<sup>1,2</sup>

<sup>1</sup>*Institute of Atomic and Molecular Physics, Jilin University, Changchun 130012, China*

<sup>2</sup>*Jilin Provincial Key Laboratory of Applied Atomic and Molecular Spectroscopy (Jilin University), Changchun 130012, China*  
(Received 7 October 2015; revised 28 January 2016; accepted 23 February 2016)

## Abstract

The ultrafast dynamic process in semiconductor Ge irradiated by the femtosecond laser pulses is numerically simulated on the basis of van Driel system. It is found that with the increase of depth, the carrier density and lattice temperature decrease, while the carrier temperature first increases and then drops. The laser fluence has a great influence on the ultrafast dynamical process in Ge. As the laser fluence remains a constant value, though the overall evolution of the carrier density and lattice temperature is almost independent of pulse duration and laser intensity, increasing the laser intensity will be more effective than increasing the pulse duration in the generation of carriers. Irradiating the Ge sample by the femtosecond double pulses, the ultrafast dynamical process of semiconductor can be affected by the temporal interval between the double pulses.

**Keywords:** carrier; energy transfer; femtosecond laser; lattice; semiconductor

## 1. Introduction

The interaction between ultrashort laser pulses and semiconductor materials has been the hot topic in the past two decades and it has been well investigated both experimentally<sup>[1–6]</sup> and theoretically<sup>[6–11]</sup>. Since the ultrashort laser pulses cause minimal collateral damage to the surrounding material, it can find extensive applications in micromachining, nanostructuring, etc.<sup>[12–14]</sup>.

Presently, the mechanism of momentum and energy relaxation, carrier–carrier scattering, valley–valley scattering, optical phonon scattering and the microscopic process during carrier diffusion have been investigated<sup>[15–17]</sup>. As the semiconductor is irradiated by ultrashort laser pulses, if the photon energy is larger than the band gap of semiconductor, the electrons within the absorption depth will transit from the valence band to the conduction band through the multiphoton absorption process, generating holes in the valence band at the same time. These non-equilibrium carriers (electron–hole pairs) will couple with the lattice system temporally and spatially, and finally most of their energy is transferred to the lattice; as a result, the system regains thermal equilibrium by assigning the heat between the carriers and lattices<sup>[1, 3]</sup>. This is an ultrafast process which occurs in

several picoseconds. The smaller the size of semiconductor device, the shorter its response time is; therefore, it is crucial to have a clear understanding for the dynamical energy transfer process occurred inside the semiconductor devices over an ultrashort time. Generally, much attention has been paid to the understanding of the dynamics of the non-equilibrium carriers, and it is commonly believed that non-equilibrium phonon effects can affect the release and delivery of the hot carriers<sup>[18, 19]</sup>. In practice, the number of non-equilibrium phonons has been measured through the Raman scattering method, demonstrating the existence of non-equilibrium phonons generated by hot carriers<sup>[20–24]</sup>. Hu *et al.* used the van Driel system<sup>[23–25]</sup> to study the change of carrier concentration, lattice temperature with the pulse duration, and found that carrier density and lattice temperature at the surface of semiconductor rise with the increase of pulse duration, which is in good agreement with the experimental results<sup>[17, 26]</sup>. However, the dynamical process inside the semiconductor is less investigated<sup>[27]</sup>, and it will be investigated in present work.

In this paper, the ultrafast dynamical process of semiconductor Ge irradiated by the femtosecond laser pulses is simulated by solving density-dependent two temperature model (DDTTM) proposed by van Driel<sup>[23–25]</sup>. The influence of pulse duration, intensity and fluence on the time evolution of carrier density and lattice temperature at the different depths

Correspondence to: S. Li and M. Jin, No. 2699, Qianjin Avenue, Changchun, Jilin, CN 130012, China. Email: [suyu11@mails.jlu.edu.cn](mailto:suyu11@mails.jlu.edu.cn), [mxjin@jlu.edu.cn](mailto:mxjin@jlu.edu.cn)

in Ge is investigated. To further investigate the effect of pulse duration on the ultrafast dynamical process of Ge, the femtosecond double-pulse technique is adopted in the end.

## 2. Theoretical model

The ultrafast dynamical process of semiconductor can be simulated by numerically solving the DDTM<sup>[23–25]</sup> or the multiple rate equation (MRE)<sup>[28]</sup>. In our work, we just carry out the simulation via the DDTM model. This model involves four coupled differential equations for the space-time evolution of carrier (hole–electron pairs) density  $N$  and the temperature of electron ( $T_e$ ), hole ( $T_h$ ) and lattice ( $T_l$ ). Assuming that the particles are in local thermodynamic equilibrium, the carrier and thermal transport,  $N$ ,  $T_e$ ,  $T_h$  and  $T_l$  is given by the following equations<sup>[24, 25]</sup>:

$$\frac{\partial N}{\partial t} = -\nabla \cdot J + G + R_A, \quad (1)$$

$$C_L \frac{\partial T_l}{\partial t} = -\nabla \cdot W_l + L_e + L_h, \quad (2)$$

$$\frac{\partial U_e}{\partial t} = -\nabla \cdot W_e + S_e - L_e - L_{e \rightarrow h}, \quad (3)$$

$$\frac{\partial U_h}{\partial t} = -\nabla \cdot W_h + S_h - L_h - L_{e \rightarrow h}, \quad (4)$$

where  $R_A$  is the net recombination rate which is given by  $-\gamma N^3$  with Auger recombination coefficient  $\gamma$ ,  $G$  accounts for the carrier generation rate and  $J$  refers to the particle current.  $S_e$  and  $S_h$  represents the energy source terms for electrons and holes.  $L_e$ ,  $L_h$  and  $L_{e \rightarrow h}$  are the energy transfer terms between electrons and phonons, holes and phonons, and electrons and holes.  $U_e$  and  $U_h$  are the fluence for electrons and holes, and  $W_e$ ,  $W_h$  and  $W_l$  are the energy currents for electrons, holes and the lattice, respectively.  $C_l$  is the lattice thermal conductivity.

Equations (1)–(4) are four coupled 1D differential equations. The spot of laser beam on samples is around 30  $\mu\text{m}$  in diameter, while the carrier diffusion length ( $\sim 0.1 \mu\text{m}$ ) is much less than the size of the laser spot within the picosecond time domain. As a result, the carriers will diffuse mainly into bulk because of the large vertical carrier density gradient. For this reason, 1D model is enough to describe the interaction between femtosecond laser pulse and Ge. In the following part, we use the variable  $z$  to denote the thickness direction.

The particle current  $J$  in Equation (1) can be calculated as:

$$J = -D \left[ \nabla N + \frac{N}{k_B T_{eh}} \nabla E_g + \frac{N}{T_{eh}} (\nabla T_e + \nabla T_h) \right], \quad (5)$$

where  $E_g$  is the energy band gap of Ge,  $k_B$  is the Boltzmann constant and  $D$  is the ambipolar diffusion coefficient which

**Table 1.** Parameters of  $G_e$  at temperature of 300 K<sup>[24]</sup>.

Parameter	Value
Density $\rho$	5.32 g/cm <sup>3</sup>
Lattice thermal conductivity $k_l$	0.6 W/(cm · K)
Lattice specific heat $C_l$	1.7 J/(K · cm <sup>3</sup> )
Auger recombination rate $\gamma$	$2 \times 10^{-31}$ cm <sup>6</sup> /s
Band gap $E_g$	0.664 eV
Electron effective mass $\dot{m}_e$	0.22 $m_0$
Hole effective mass $\dot{m}_h$	0.34 $m_0$
Electron mobility $\mu_e$	3800 cm <sup>2</sup> /(V · s)
Hole mobility $\mu_h$	1800 cm <sup>2</sup> /(V · s)
Electron diffusivity $D_e^0$	103 cm <sup>2</sup> /s
Hole diffusivity $D_h^0$	54 cm <sup>2</sup> /s
Absorption coefficient $\alpha$ (620 nm)	$1.9 \times 10^5$ cm <sup>-1</sup>
Reflectivity $R$ (620 nm)	0.5
Electron optical deformation $d_e^0$	$6.4 \times 10^{-4}$ erg/cm
Hole optical deformation $d_h^0$	$14.0 \times 10^{-4}$ erg/cm

is associated with carrier temperature<sup>[23–25]</sup>:

$$D = D_e^0 D_h^0 \left\{ \frac{T_e + T_h}{D_h^0 T_e + D_e^0 T_h} \right\}, \quad (6)$$

where  $D_e^0 \propto T_e^{1/2}$  and  $D_h^0 \propto T_h^{1/2}$  are the Maxwell–Boltzmann electron and hole diffusion constants appropriate for the ambient temperature. The carrier generation rate under the action of a Gaussian laser pulse is given as

$$G(z, t) = \frac{(1 - R)\alpha I_0(t)e^{-\alpha z}}{\hbar\omega_0}, \quad (7)$$

where  $R$  is the optical reflectivity,  $I_0(t) = I_0 e^{-4 \ln 2 (t/\tau)^2}$  refers to the laser intensity, and  $\tau$  denotes the pulse duration. In our simulation, the wavelength of the laser pulse used to irradiate sample is  $\lambda = 620$  nm; since the photon energy  $\hbar\omega_0$  (2 eV) is much larger than the band gap energy of  $G_e$ , the electron can transit from the valence band to the conduction band by absorbing only one photon. For this reason, multi-photon absorption process can be ignored.  $\alpha$  is the one photon absorption coefficient. It should be noted that  $R$  and  $\alpha$  are density-dependent<sup>[27, 29, 30]</sup>; therefore, to model the dynamical process of Ge irradiated by the femtosecond laser more accurately,  $R$  and  $\alpha$  should be dynamic. However, for the convenience of research, we just consider them as constant values (see Table 1), which can qualitatively describe the interaction between femtosecond laser and Ge. Using conservation of energy and momentum in the absorption process, the energy generation ratio for electrons  $S_e$  and holes  $S_h$  can be calculated from  $G(z, t)$ :

$$S_e(z, t) = \frac{\dot{m}_h}{\dot{m}_h + \dot{m}_e} G(z, t) \cdot (\hbar\omega_0 - E_g), \quad (8)$$

$$S_h(z, t) = \frac{\dot{m}_e}{\dot{m}_h + \dot{m}_e} G(z, t) \cdot (\hbar\omega_0 - E_g), \quad (9)$$

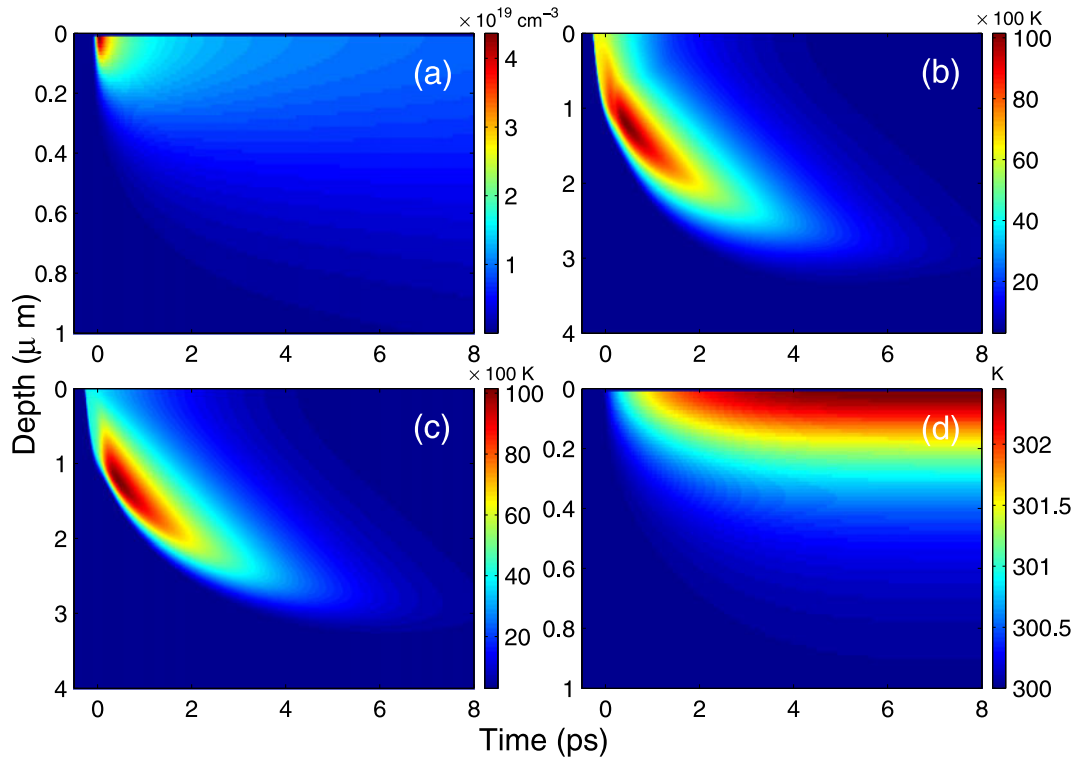


**Figure 1.** Time-space evolution of (a)  $N$ , (b)  $T_e$ , (c)  $T_h$  and (d)  $T_l$  in Ge irradiated by laser pulse whose duration, wavelength and fluence are 100 fs, 620 nm and  $0.1 \text{ mJ/cm}^2$ , respectively.

where  $m_e$  and  $m_h$  are the effective masses of electron and holes.

The energy current for electrons, holes and lattice system is given by:

$$W_e = J [E_c + 2K_B T_e] - \kappa_e \nabla T_e, \quad (10)$$

$$W_h = J [E_v + 2K_B T_h] - \kappa_h \nabla T_h, \quad (11)$$

$$W_l = -\kappa_l \nabla T_l, \quad (12)$$

where  $E_c$  and  $E_v$  are potential energies of conduction band and valence band;  $\kappa_e$ ,  $\kappa_h$  and  $\kappa_l$  are the thermal conductivity coefficients for electrons, holes and lattice phonons, respectively. After photo-excitation, electrons and holes possess kinetic energy. The total fluence of the electrons  $U_e$  and holes  $U_h$  are functions of carrier density  $N$  and  $T_e$ ,  $T_h$ , which can be calculated according to the following expressions:

$$U_e = N E_c + \frac{3}{2} N k_B T_e, \quad (13)$$

$$U_h = N E_v + \frac{3}{2} N k_B T_h. \quad (14)$$

For the sake of simplicity, here we just present the main content of the DDTM; for more detailed information, please refer to Ref. [23–25].

From the above descriptions, we know that Equations (1)–(4) are four coupled nonlinear diffusion equations, and quantities  $N$ ,  $T_e$ ,  $T_h$  and  $T_l$  are all functions of each other. To

numerically solve these equations, good numerical schemes are needed. It is known that finite-difference methods is among the most effective ones to solve the nonlinear differential equations<sup>[31]</sup>. The finite-difference methods can be divided into several kinds, including implicit and explicit difference scheme, and Crank–Nicholson scheme. Considering comprehensively the computational speed, accuracy and stability of different schemes, in our simulation the code is written by the combination of implicit and explicit difference scheme. The diffusion terms, i.e.,  $\partial^2 N / \partial z^2$  and  $\partial^2 T / \partial z^2$ , must be processed by the implicit difference scheme, while the other terms, such as  $\partial N / \partial z$ ,  $\partial N / \partial t$ ,  $\partial T / \partial z$  and  $\partial T / \partial t$ , must be processed by the explicit difference scheme.

### 3. Results and discussion

The semiconductor Ge at the room temperature (300 K) is taken as the computational example, and the ultrafast dynamical process under femtosecond laser pulses is investigated. The initial carrier density is selected as  $N_0 \cong 10^{12} \text{ cm}^{-3}$ . Figure 1 shows the change of  $N$ ,  $T_e$ ,  $T_h$  and  $T_l$  in Ge with time and depth. For the femtosecond laser used, its central wavelength, duration and fluence are 620 nm, 100 fs and  $0.1 \text{ mJ/cm}^2$ , respectively. Since the photon energy is larger than the band gap of Ge, the electron will be excited from the valence band to conduction band when the Ge sample is

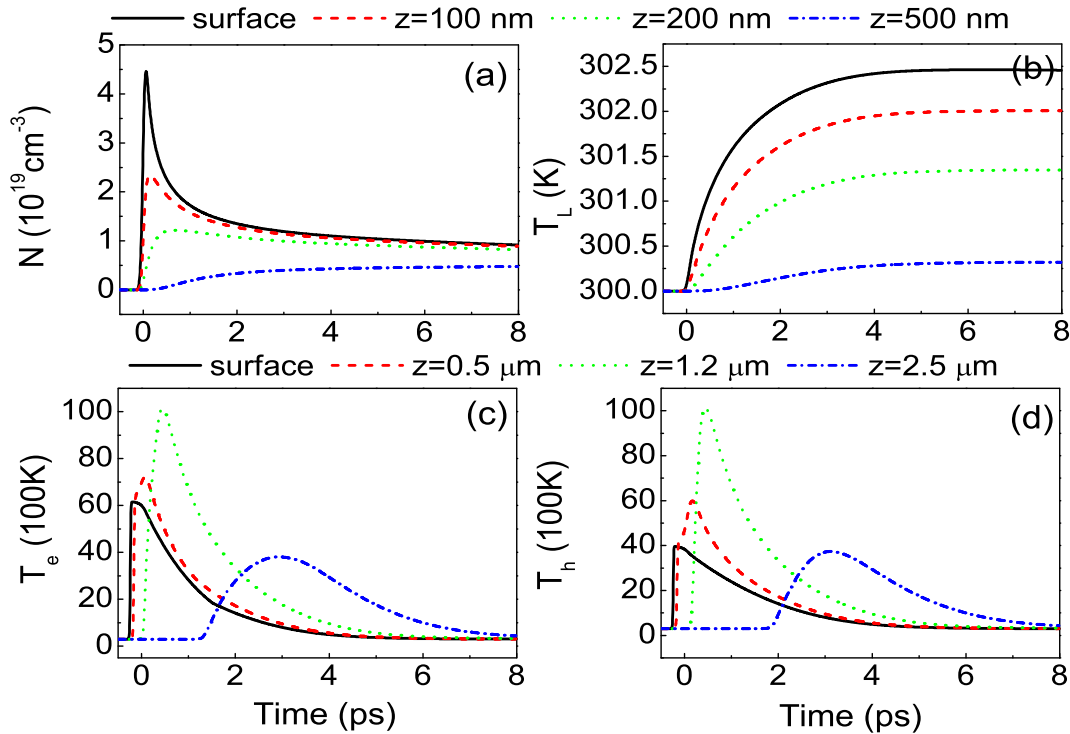


**Figure 2.** Time evolution of (a)  $N$ , (b)  $T_L$  (c)  $T_e$  and (d)  $T_h$  in Ge at different depths.

irradiated by the laser pulse, and holes with the same quantity will be generated at the same time, thereby generating a great number of carrier pairs. On the other hand, the electron in the conduction band will recombine with the hole via the Auger recombination whose rate  $R_A$  depends on  $N^3$ . As  $N$  reaches the critical value, the carrier pairs recombined will be more than those generated, resulting in the decrease of  $N$ . Therefore, with the increase of time,  $N$  first increases and then drops. In addition,  $N$  decreases greatly with the increase of depth, as shown in Figure 1(a). It can be seen from Figures 1(b) and (c) that the temporal behavior of carrier temperature  $T_c$  is same as that of  $N$ ; however, with the increase of depth,  $T_c$  also increases first and then decreases. As is shown in Figure 1(d),  $T_l$  increases with time slowly and decreases with increasing depth. What is more,  $T_l$  change in a small scope, and we can see from the figure that  $T_l$  stays at 302.5 K at the surface of Ge, which changes as less as 2.5 K.

To make a more clear comprehension of the above phenomena, in Figure 2, we present the temporal evolution of  $N$ ,  $T_e$ ,  $T_h$  and  $T_l$  in Ge for several specific depths selected from Figure 1. It can be seen from the solid black curves in Figure 2 that a great number of carrier pairs are generated at the surface of Ge under femtosecond laser irradiation, and the temperature of these carriers rises by absorbing plenty of energy. The electron will recombine with hole via the Auger recombination and simultaneously transfer the energy and momentum to another electron (hole) nearby, which is a nonradiative process. Consequently, the electron (hole) nearby is excited to the higher states

inside the conduction (valence) band<sup>[32–35]</sup>. As a result, the electron (hole) temperature increases<sup>[33, 34]</sup>. The electrons with enough kinetic energy can knock the electrons in the valence band and promote them to higher states in the conduction band, creating new electron–hole pairs, which is the impact ionization process<sup>[36–38]</sup>. It will repeat the above process until the thermal equilibrium is reached. Moreover, part of energy is transferred from the carrier to the lattice via the electron–phonon interaction in this process, increasing  $T_l$ , as shown in Figure 2(b); however, the mean kinetic energy of carrier is always higher than that of the lattice, and we can know from  $E_k \propto k_B T$  that  $T_e$  and  $T_h$  are always higher than  $T_l$ . Whereas, with the increase of depth and time, the temperature difference between the carrier and lattice decreases and finally a thermal equilibrium is reached. After undergoing such a time-space evolution process, the energy is finally transferred to the interior of Ge.

The laser pulse can penetrate into the interior of semiconductor, and for Ge, the skin depth (i.e., penetration depth) is  $\delta = 1/\alpha \approx 50 \text{ nm}$ . Along with the increase in depth, the energy penetrated decreases exponentially. Though energy can be transferred to the interior of Ge via the Auger recombination and impact ionization, it still decreases greatly; therefore, fewer carrier pairs can be generated at a deeper place, as shown in Figure 2(a). As fewer carrier pairs are generated, the energy transferred from the carrier to the lattice via the electron–phonon interaction decreases correspondingly, leading to the decrease of  $T_L$  with increasing depth, as shown in Figure 2(b). During the Auger

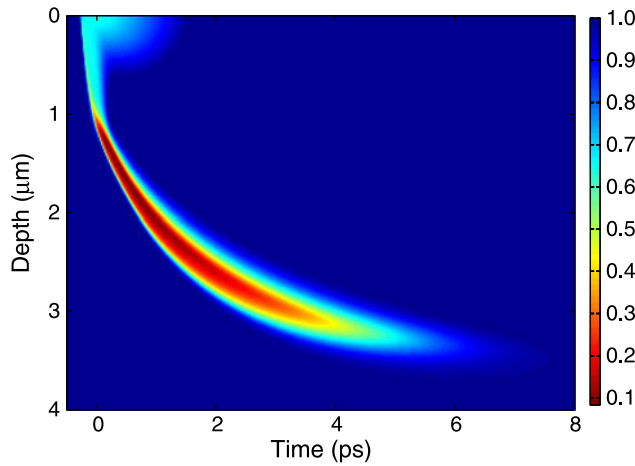


**Figure 3.** Time-space evolution of the value of  $T_h/T_e$ . The pulse duration and fluence is 100 fs, and  $0.1 \text{ mJ/cm}^2$ , respectively.

recombination, a three-body interaction occurs: two carriers recombine and a third carrier takes up the recombination energy. The Auger recombination makes  $N$  lower, and

increases the kinetic energy of new-generated carriers at the same time. As a result, energy will be accumulated at the interior of Ge, resulting in the increase of  $T_e$  and  $T_h$  with increasing depth, and here we name it ‘energy accumulation effect’. However, part of carriers’ kinetic energy is transferred to lattice simultaneously. As it reaches a certain depth, the energy accumulated by the carrier pairs becomes less than that transferred from the carrier pairs to the lattice, lowering carrier temperature  $T_c$ . Therefore, with the increase of depth,  $T_c$  first increases and then decreases, as shown in Figure 2(c) and (d).

It can be also seen from Figures 2(c) and (d) that there is a great difference between the temporal behaviors of  $T_e$  and  $T_h$ . In Figure 3, we present time-space evolution of  $T_h/T_e$ . From the figure we can see that both the temporal and spatial behaviors of  $T_e$  and  $T_h$  show difference during the energy transport in semiconductor. In order to analyze the energy transfer between electron and hole more distinctly, we select from Figures 1(b) and (c) the spatial evolution of  $T_e$  and  $T_h$  in Ge at  $-0.21, 0.0, 0.2, 1.0, 2.5$  and  $8.0 \text{ ps}$ , as shown in Figure 4. Irradiated by the femtosecond laser,

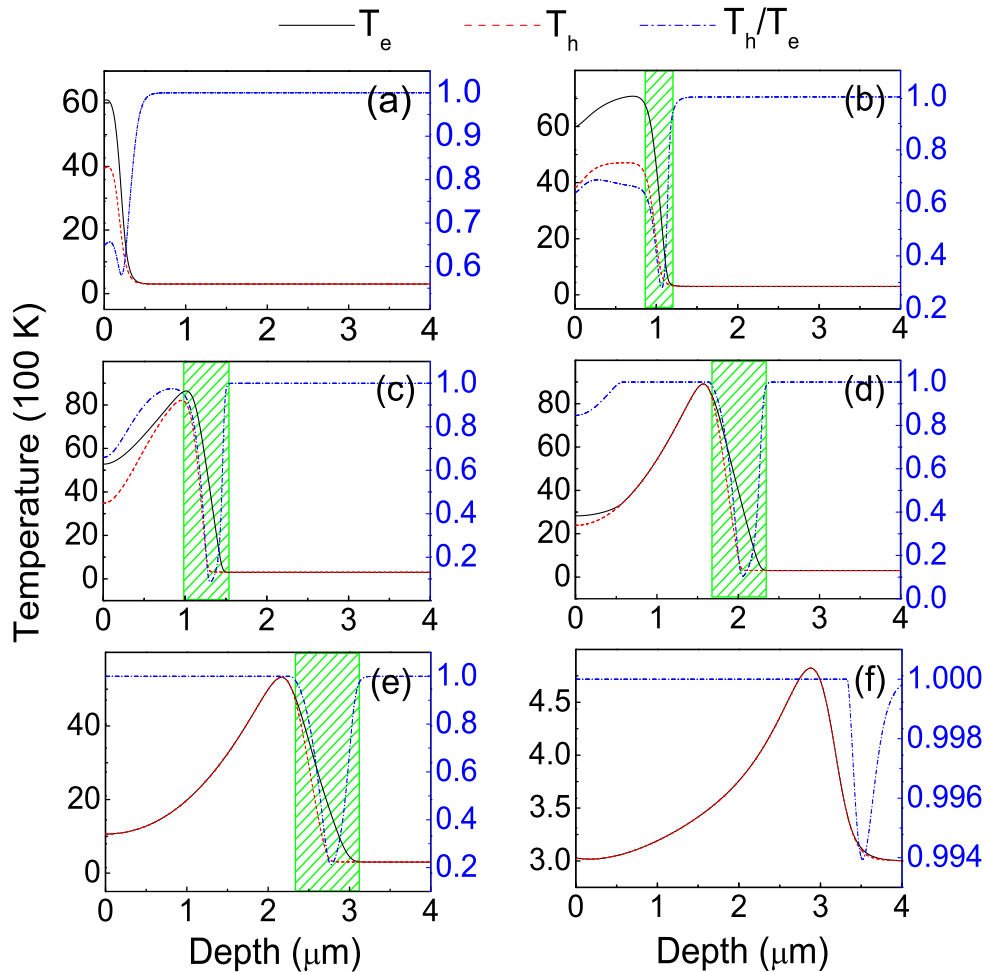


**Figure 4.** Spatial evolution of  $T_e$ ,  $T_h$  and  $T_h/T_e$  (right axis) at (a) 0.21, (b) 0, (c) 0.2, (d) 1.0, (e) 2.5 and (f) 8.0 ps.



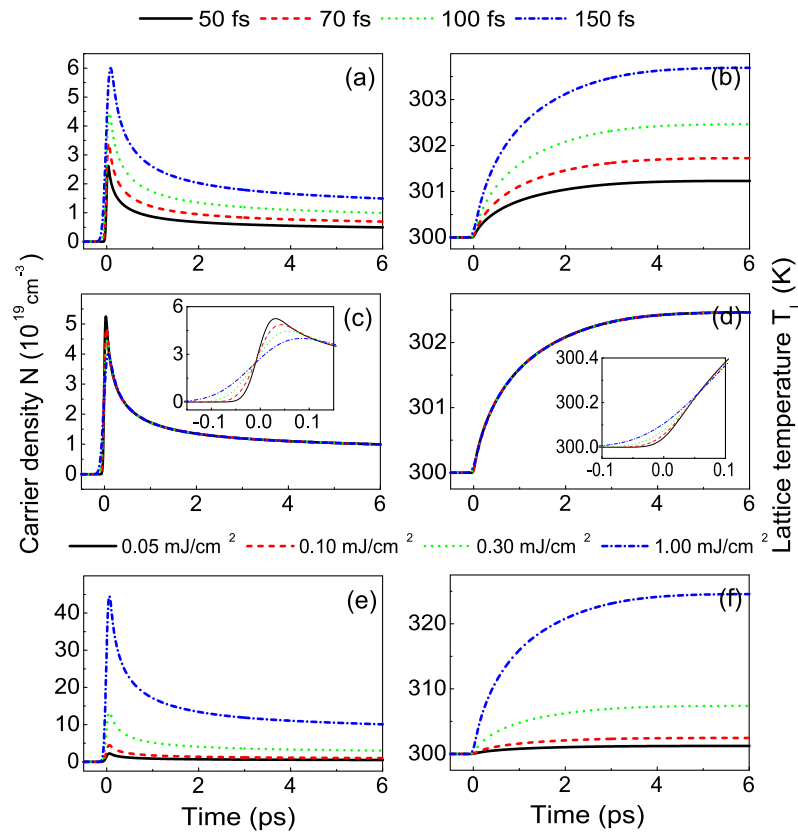


**Figure 5.** Time evolution of (a, c, e)  $N$  (b, d, f)  $T_L$  in Ge irradiated by laser pulses (a, b) with different durations and same intensity  $I_0$  ( $798 \text{ MW/cm}^2$ ); (c, d) with different durations and same fluence ( $0.1 \text{ mJ/cm}^2$ ) and (e, f) with different energy densities and same duration ( $100 \text{ fs}$ ).

both  $T_e$  and  $T_h$  increase rapidly and at  $t = -0.21 \text{ ps}$ , they reach their maxima at the surface of Ge, which are  $6157$  and  $3961 \text{ K}$  (see the solid black curves in Figures 2(c) and (d)). Since the effective mass of electron is smaller than that of hole, from requirements of momentum and energy conservation, the kinetic energy of hole generated  $E_k^h$  will be smaller than that of the corresponding electron  $E_k^e$ , and the relation between them is  $E_k^h/E_k^e = \dot{m}_e/\dot{m}_h$ . Therefore,  $T_e$  is higher than  $T_h$  and thus  $T_h/T_e$  is much lower than 1 at some depths, which can be clearly seen from the dash-dotted blue curves in Figure 4. Due to the accumulation of carriers' kinetic energy, the carrier temperature at the interior is higher than that at the surface, as shown in Figures 4(b) and (c). At  $t = 0.2 \text{ ps}$ , the laser irradiation terminates, at the surface of Ge,  $T_e$  and  $T_h$  begin to decrease, while at the interior, the difference between the maximum values of  $T_e$  and  $T_h$  becomes smaller, as shown in Figure 4(c). However, beyond the depth corresponding to maximum value, with the increase of depth,  $T_h$  decays more obviously than  $T_e$ , and thus the value of  $T_h/T_e$  decreases much, as shown by the green areas in the Figures 4(b–e), indicating that the energy can be transferred to electron at deeper place at the same moment. These green areas correspond to the low  $T_h/T_e$  values in Figure 3. What is more, Figures 2(c), (d) show that the  $T_e$  increases earlier than  $T_h$ , indicating that the electron

plays a more significant role than hole in the energy transport in semiconductor. As time evolves,  $T_e$  and  $T_h$  gradually tend to be the same at different depths [Figures 4(d–f)] and become nearly the same after  $7 \text{ ps}$ ; consequently, the thermal equilibrium between electron and hole is reached eventually, as shown in Figures 3 and 4(f).

For the temporally Gaussian type laser pulse used, its fluence  $F$  is related to duration  $\tau$  through  $F = \sqrt{\pi/2}\tau I_0$ . For this reason, the ultrafast dynamical process in semiconductor may be affected by three factors: laser fluence  $F$ , pulse duration  $\tau$  and intensity  $I_0$ . In the following, in the case that the value of one factor is fixed, the influence of the other two factors on  $N$  and  $T_L$  at the surface of Ge will be investigated. Figures 5(a) and (b) shows the time evolution of  $N$  and  $T_L$  in Ge irradiated by the laser pulses whose durations are  $50$ ,  $70$ ,  $100$  and  $150 \text{ fs}$ , respectively. The intensity is fixed as  $I_0 = 798 \text{ MW/cm}^2$ . It can be seen from the figure that both  $N$  and  $T_L$  increase with the increase of pulse duration, which can be attributed to the fact that as the pulse duration is larger, more energy is involved in the interaction between the laser pulses and semiconductor; therefore, more carrier pairs can be generated. Consequently, more carrier's kinetic energy can be transferred to lattice via the electron–phonon interaction, thereby increasing its temperature. Figures 5(c) and (d) shows the temporal evolution of  $N$  and  $T_L$  in Ge

irradiated by the femtosecond laser pulses whose durations are same as those in Figures 5(a) and (b), and the fluence is fixed as  $F = 0.1 \text{ mJ/cm}^2$  (in this case,  $I_0$  is in inverse proportion to  $\tau$ ). From the figure we can see that the temporal behaviors of  $N$  and  $T_l$  are almost independent of the incident pulse duration as well as the laser intensity. However, we can see from the insert in Figure 5(c) that along with the increase of the incident pulse duration, the instant at which the carrier pairs are generated is put ahead, making  $T_l$  begin to rise in advance (see the insert in Figure 5(d)), while the maximum value of  $N$  decreases and appears later. The above discussions indicate that the evolution of  $N$  and  $T_l$  can be determined by laser fluence, namely the total energy. To further verify this conclusion, we present in Figures 5(e) and (f) the temporal behaviors of  $N$  and  $T_l$  in Ge irradiated by the laser pulses whose fluences are 0.05, 0.10, 0.30 and 1.00 mJ/cm, and the duration is fixed as 100 fs. It can be seen from the figure that along with the increase of laser fluence, both  $N$  and  $T_l$  increase greatly.

In practice, in Figures 5(a) and (b), the fluence is also increased as the pulse duration increases, which is in a way similar to the case in Figures 5(e) and (f). Therefore, there are two ways to increase the laser fluence; path A: increasing intensity in the case of fixed pulse duration, and path B: increasing pulse duration in the case of fixed intensity. However, we can see from the insert in Figure 5(c) that as the fluence is fixed, the maximum value of  $N$  ( $N_{\max}$ ) decreases with increasing pulse duration. To clearly show this phenomenon, we present in Figure 6 the variation of  $N_{\max}$  with laser fluence which is increased by the two ways. In path A, the pulse duration is fixed as 50 fs and the intensity is increased from  $I_0 = 798 \text{ MW/cm}^2$  to  $I_0 = 7980 \text{ MW/cm}^2$ , while in path B, the intensity is fixed as  $I_0 = 798 \text{ MW/cm}^2$  and the pulse duration is increased from 50 to 500 fs. It can be seen from the figure that  $N_{\max}$  in the case of path A is larger than that in the case of path B. This phenomenon is caused by the fact that even at the same fluence, as the pulse duration is longer, part of the energy has already transferred to the interior of the semiconductor when the peak of the pulse irradiates it, and the decrease in energy at the surface will result in the generation of less carriers.

From the above study we know that when the carrier density  $N$  reaches the maximum, it will take a relatively long time (several picoseconds) to decrease to a relatively low value. If an addition femtosecond pulse is imposed on the semiconductor shortly after  $N$  begins to decrease, can the ultrafast dynamical process of semiconductor be affected? In the following, we impose another pulse with same intensity ( $I_0 = 798 \text{ MW/cm}^2$ ) but different duration on the semiconductor so as to study the temporal evolution of  $N$  and  $T_l$  at the surface of Ge, and the temporal interval between the two pulses is 100 fs, as shown in Figures 7(a) and (b). It can be seen from figure that compared with the case of single pulse (solid black curves), under the irradiation of femtosecond double pulses,  $N$  and  $T_l$  in Ge increase

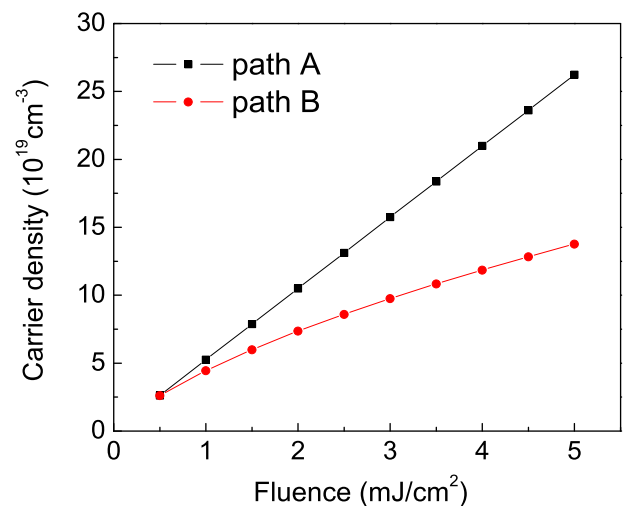


**Figure 6.** Variation of the maximum value of  $N$  with increasing fluence. The fluence is increased by the two ways: path A (increasing intensity in the case of fixed pulse duration) and path B (increasing pulse duration in the case of fixed intensity).

significantly, and the longer the second pulse, the higher the values of  $N$  and  $T_l$  are. This phenomenon is caused by the fact that  $N$  and  $T_l$  in Ge have not changed much when the second pulse is added, in which case the energy accumulation effect still plays the dominant role; the longer the second pulse, the more the energy will be accumulated, as a result, more carrier pairs can be generated and thus more energy can be transferred to the lattice via the electron-phonon interaction. In addition, the time interval between the double pulses can also influence the evolution of  $N$  and  $T_l$ . If the interval is relative large, say  $\Delta T = 400 \text{ fs}$ , before the second pulse is imposed,  $N$  has already decreased much [dash-dotted blue curve in Figure 7(c)] and plenty of energy has been transferred to the lattice; consequently,  $N_{\max}$  becomes smaller than that as the interval is smaller, say  $\Delta T = 50 \text{ fs}$  [solid black curve in Figure 7(c)] and the increase tendency of  $T_l$  becomes weaker. However, since the total energy of the double pulses is independent of the time interval between them, the temporal behaviors of  $N$  and  $T_l$  tend to be same in all cases eventually, as shown in Figures 7(c) and (d).

#### 4. Conclusion

In this paper, taken the semiconductor Ge as the research object, we simulate the energy transport process at the surface and interior of Ge which interacts with the femtosecond laser pulses. By investigating the evolution of carrier density, carrier and lattice temperature, it is found that as the depth increases, the carrier density and lattice temperature decrease, while the carrier temperature first increases and then decreases, and this can be attributed to

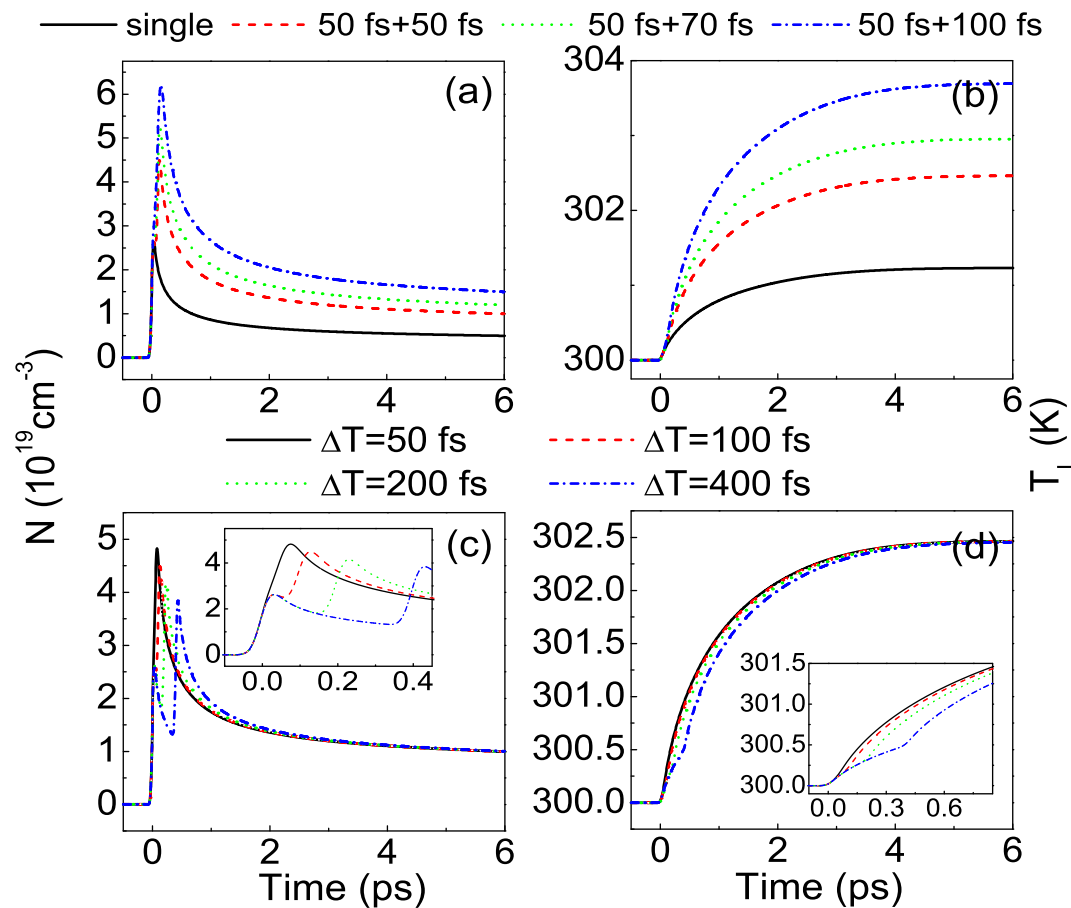


**Figure 7.** Time evolution of (a)  $N$  and (b)  $T_L$  in Ge irradiated by double pulses, where the interval between them is 100 fs, the duration of the first pulse is 50 fs and that of the second one is 50, 70 and 100 fs, respectively; time evolution of (c)  $N$  and (d)  $T_L$  in Ge irradiated by the double pulses, where the duration of them are both 50 fs, and the interval between them is 50, 100, 200 and 400 fs, respectively.

the competition between energy accumulation effect and energy transfer from carrier to lattice via the electron-phonon interaction. The energy can be transferred to the interior of semiconductor via the Auger recombination and impact ionization. The ultrafast dynamical process in Ge is greatly affected by the laser fluence, while in the case of fixed fluence, the overall evolution of the carrier density and lattice temperature is nearly independent of pulse duration and laser intensity. However, increasing the laser intensity will be more effective than increasing the pulse duration in the generation of carriers. In the end, irradiating the Ge sample by femtosecond double pulses, it is found that the ultrafast dynamical process of semiconductor can be affected by the time interval of the double pulses.

### Acknowledgements

This work is supported by the National Basic Research Program of China (973 Program, grant no. 2013CB922200), the National Natural Science Foundation of China (grant no. 11474129), the Research Fund for the Doctoral Program of

Higher Education in China (grant no. 20130061110021) and the Project 2015091 Supported by Graduate Innovation Fund of Jilin University.

### References

1. J. S. Preston and H. M. van Driel, *Phys. Rev. B* **30**, 1950 (1984).
2. X. Y. Wang, D. M. Riffe, Y. S. Lee, and M. C. Downer, *Phys. Rev. B* **50**, 8016 (1994).
3. T. Sjodin, H. Petek, and H. L. Dai, *Phys. Rev. Lett.* **81**, 5664 (1998).
4. N. M. Bulgakova and A. V. Bulgakov, *Appl. Phys. A* **73**, 199 (2001).
5. A. J. Sabbah and D. M. Riffe, *Phys. Rev. B* **66**, 165217 (2002).
6. L. Englert, M. Wollenhaupt, L. Haag, C. Sarpe-Tudoran, B. Rethfeld, and T. Baumert, *Appl. Phys. A* **92**, 749 (2008).
7. B. Rethfeld, *Phys. Rev. Lett.* **92**, 187401 (2004).
8. P. Allenspacher, B. Huttner, and W. Riede, *Proc. SPIE* **4932**, 358 (2003).
9. N. M. Bulgakova, R. Stoian, A. Rosenfeld, I. V. Hertel, and E. E. B. Campbell, *Phys. Rev. B* **69**, 054102 (2004).
10. N. M. Bulgakova, R. Stoian, A. Rosenfeld, I. V. Hertel, W. Marine, and E. E. B. Campbell, *Appl. Phys. A* **81**, 345 (2005).



11. D. Autrique, G. Clair, D. L. Hermite, V. Alexiades, A. Bogaerts, and B. Rethfeld, *J. Appl. Phys.* **114**, 023301 (2013).
12. L. W. James, J. P. van Dyke, F. Herman, and D. M. Chang, *Phys. Rev. B* **1**, 3998 (1970).
13. A. Voge and V. Venugopalan, *Chem. Rev.* **103**, 577 (2003).
14. D. Bauerle, *Laser Processing and Chemistry*, 4th edn (Springer, Berlin, 2011).
15. M. Li, K. Mori, M. Ishizuka, X. Liu, Y. Sugimoto, N. Ikeda, and K. Asakawa, *Appl. Phys. Lett.* **83**, 216 (2003).
16. J. Shah, T. C. Damen, W. T. Tsang, A. C. Gossard, and P. Lugli, *Phys. Rev. Lett.* **59**, 2222 (1987).
17. X. F. Hu and M. C. Downer, *Ultrafast Phenomena IX*, Springer Series in Chemical Physics, vol. 60, p. 344 (1994).
18. M. I. Gallant and H. M. van Driel, *Phys. Rev. B* **26**, 2133 (1982).
19. H. V. van Driel, *Phys. Rev. B* **19**, 5928 (1979).
20. N. Potz and P. Kocevar, *Phys. Rev. B* **28**, 7040 (1983).
21. D. von der Linde, J. Kuhl, and H. Klingenberg, *Phys. Rev. Lett.* **44**, 1505 (1980).
22. J. A. Kash, J. C. Tsang, and J. M. Hvam, *Phys. Rev. Lett.* **54**, 2151 (1985).
23. A. Othonos, H. M. van Driel, J. F. Young, and P. J. Kelly, *Solid-State Electron.* **32**, 1573 (1988).
24. H. M. Van Driel, *Phys. Rev. B* **35**, 8166 (1987).
25. A. Othonos, H. M. van Driel, J. F. Young, and P. J. Kelly, *Phys. Rev. B* **43**, 6682 (1991).
26. H. R. Choo, X. F. Hu, M. C. Downer, and V. P. Kesan, *Appl. Phys. Lett.* **63**, 1507 (1993).
27. Y. Gan and J. K. Chen, *Appl. Phys. A* **105**, 427 (2011).
28. D. Lenstra and M. Yousefi, *Opt. Express* **22**, 8143 (2014).
29. K. Sokolowski-Tinten and D. von der Linde, *Phys. Rev. B* **61**, 2643 (2000).
30. N. Medvedev and B. Rethfeld, *J. Appl. Phys.* **108**, 103112 (2010).
31. G. P. Agrawal, *Nonlinear Fiber Optics*, 3rd edn p. 55 (Academic Press, 2001).
32. R. A. Abram, R. W. Kelsall, and R. T. Taylor, *J. Phys. Chem. Solids* **49**, 607 (1988).
33. M. Takeshima, *J. Appl. Phys.* **58**, 3846 (1985).
34. P. Borri, S. Ceccherini, M. Gurioli, and F. Bogani, *Solid State Commun.* **103**, 77 (1997).
35. M. Achermann, A. P. Bartko, J. A. Hollingsworth, and V. I. Klimov, *Nat. Phys.* **2**, 557 (2006).
36. L. V. Keldysh, *Sov. Phys. JETP* **21**, 1135 (1965).
37. J. Bude and K. Hess, *Phys. Rev. B* **45**, 10958 (1991).
38. H. Tanimura, J. Kanasaki, and K. Tanimura, *Sci. Rep.* **4**, 6849 (2014).